MHD Mixed Convection-Radiation Interaction in Porous Medium within a Rough Channel with Navier and Thermal Slip

P. F. Fasogbon

Abstract— This work is focused on the modeling of the problem on steady, laminar, mixed-convection flow of a viscous incompressible, electrically conducting dissipative fluid through porous medium between cool sinusoidal roughened wall and a hot parallel flat wall in the presence of radiative heat transfer in an optically thin environment, taking fluid temperature gradient dependent heat generation into account. The fluid is assumed to satisfy thermal and velocity slip boundary conditions on the wall. The dimensionless governing equations are perturbed and then solved numerically; utilizing mid-point method with Richardson Extrapolation (MMRE) by software MAPLE. Impacts of key non-dimensional parameters on axial velocity u, secondary velocity v and temperature θ profiles have been analysed in detail and results shown graphically.

Index Terms— Finitely long vertical rough channel, magnetic and viscous dissipative fluid, mid-point method with Richardson Extrapolation (MMRE), mixed convection, porous medium, temperature gradient dependent heat generation, thermal radiation

1 Introduction

One of the most interesting and challenging areas of research in heat transfer is mixed convection flow; occurs when both forced and natural (free) convection mechanisms significantly and concurrently contribute to the heat transfer. Such flows are found in a wide range of practical applications including combustion of atomized liquid fuels, thermal-hydraulics of nuclear reactors, cooling of sophisticated electronics and heat exchanger devices, dehydration operations in chemical and food processing, flow of a cryogenic liquid in certain digital computers, and so on. Mixed convection flow of an electrically conducting fluid in sinusoidal wavy channel in the presence of magnetic field is of great importance in many industrial applications like thermal insulations, cooling of nuclear reactors, geothermal and petroleum reservoirs, and during the operations of electronic packages and micro electronic devices. In this regard, for example, Pavin et al. [1], Chauhan and Agrawal [2], and Patra et al. [3] investigated MHD mixed convection heat transfer, respectively, across vertical wavy (sinusoidal and triangular) isothermal channels and concluded that the rate of heat transfer is more effective in a sinusoidal wavy channel than in a triangular, through partially filled with clear fluid and partially filled with a fluid-saturated porous medium bounded by isothermaisoflux and isoflux-isothermal walls, and through a vertical channel with asymmetric heating of walls. Thus, Pavin et al. [1] have developed closed type of the precise answer to the geometry of present work.

Free convection heat transfer through finitely long vertical sinusoidal roughened isothermal channel have been considered by Vajravelu and Sastri [4]. An extension of the problem to hydromagnetic flow and heat transfer was studied by Fasogbon [5]. Further, Fasogbon [6] reported analytical solutions for the transfer processes governed by buoyancy mechanisms arising from both thermal and species diffusion. This was also extended to include Soret, Dufour and chemical reaction effects in the presence of a transverse magnetic field by Ghadeyan et al. [7]. In the above studies, the flows of heat or heat and mass convection have assumed classical "no-slip" boundary condition; the viscous fluid velocity is the velocity of the solid boundary. However, in some practical circumstances like wetted wall which compels fluid to slide along the wall, walls of air-craft and rockets moving at very high altitude where the particles adjacent to the wall no longer take the velocity of the wall but possess a finite tangential velocity which slips along the wall, the non-adherence of the fluid to a solid boundary known as velocity slip, is a phenomenon that has been observed. And, its impact is felt in this time of modern science, technology and ever-growing industrialization where there are many practical applications.

Accordingly, Taneja and Jain [8], Singh [9], Sengupta and Ahmed [10], Jana and Das [11] and Ibrahim and Suneetha [12] have examined MHD convection flow of various physical interest in velocity slip regime for different geometries. Amanulla et al. [13] and Nagendra et al. [14] studied the combined effects of the thermal slip (temperature jump) and hydrodynamic slip (referred to as momentum or Navier or velocity slip) on the hydromagnetic convection flow of a Williamson fluid, respectively, on the external surface of a vertical truncated cone; revealed the relevance of their work to the simulation of magnetic polymer materials processing, and on the external isothermal surface of a sphere; reported its importance to smart coating transport phenomena. Most recently, Baoku [15] examined the effects of chemical reaction, magnetic and viscous dissipation on MHD Maxwell fluid flow with two slip mechanisms (thermal and velocity slip) over a stretching sheet; relevant to the need of engineers and scien-

• *P. F. Fasogbon, Research Scholar, Department of Mathematics, Faculty of Science, Obafemi Awolowo University, 220005, Ile-Ife, Nigeria, E-mail: pfasogbon@yahoo.com, faspet@oauife.edu.ng*

tists to improve the efficiency of an upper convected Maxwell fluid flow during industrial processes. Further investigations of multiple (momentum, thermal and mass) slip mechanisms have been reported by Sekhar et al. [16] and Uddin et al. [17]. Sekhar et al. [16] studied the unsteady MHD mixed convective oscillatory flow of an optically thin fluid through a planar channel filled with saturated porous medium considering buoyancy, heat source, thermal radiation and chemical reaction effects while Uddin et al. [17] addressed the impacts of viscous and ohmic dissipation, variable transport property on MHD thermo-solutal convection in porous media; finds applications in trickle-bed reactor hydromagnetics, magnetic polymeric materials processing and MHD energy generator slip flows. Yet, the preceding literature survey shows that double wall slip phenomena on mixed convection heat transfer in heat generating electrically conducting radiating dissipative fluid through and past porous medium lead to the development of heat (energy) resources; taking temperature gradient dependent heat generations into account, confined between two finitely long vertical walls; one of which is cool sinusoidal roughened wall and the other being hot flat wall, has not being investigated and the present work demonstrate the issue.

Mixed convection flow through porous medium makes heat insulation of wall more effective to estimate its impact in heat transfer and potential use of geothermal energy for power production. Thermal hydraulics (also called thermohydraulics) is the study of hydraulic flow in the thermal fluids (e.g. steam generation in power plants). In crude oil refinery, thermohydraulic performance of refinery heat exchanger is important. Heat exchangers (basically use for heating; to lower their viscosity and cooling; to maintain the temperature of seals of pumps or compressors, of fluid) in crude oil refineries are used to transfer heat between two or more fluids, separated by solid wall(s) to prevent mixing. Now, it is desirable for engineers and scientists to add two wall slip mechanisms, for example, to sinusoidal roughness applied in heat exchangers wall(s), which is a very effective method for heat transfer enhancements and thermohydraulic performance to draw attention towards their importance for specific applications as well as minimizing the cost to moderate friction penalty, for fluid flow during industrial processes.

2 MATHEMATICAL FORMULATION

We consider the physical problem of two-dimensional ($\vec{u}=(u',v',0)$), steady, laminar mixed convection of an electrically conducting, optically thin gray gas in a porous medium between two finitely long vertical walls, hence, physical quantities now function of X and Y. The channel is characterized by a cool sinusoidal wavy wall at temperature T_c, (represented by $Y=\varepsilon^* \cos k_w X, \left|\varepsilon^*\right|<1$), and an opposite hot flat wall at temperature T_h (represented by $Y=H$). The X-axis is along the non-conducting wall taken vertically upwards and parallel to the flat wall and the Y-axis is normal to it. u', v' are the components of the velocity parallel and perpendicular to the channel length. Properties of the gas are assumed constant except that density changes with temperature that brings about the buoyancy forces in a way corresponding to the equation of state: $\rho_c=\rho[1+\beta(T-T_c)]$ There is no applied magnetic field in the Y-direction and magnetic Reynold's number is much less than unit, so that Hall, ions slip current and induced magnetic fields are neglected. $\nabla\cdot\vec{B}=0$ (Gauss's law of magnetism) gives B_y =constant= B_0 in the flow, thus $\vec{B}=(0,B_0,0)$ and Lorentz force $\vec{F}=\vec{J}\times\vec{B}=\sigma_e\left(\vec{u}\times\vec{B}\right)\times\vec{B}=-\sigma_e B^2\vec{u}$, $\nabla\times\vec{B}=\vec{J}$, $\nabla\cdot\vec{E}=0$ and $\vec{J}=\sigma_e\vec{u}\times\vec{B}$ (Ohm's law).

Maxwell currents displacement and free charges are neglected. The volumetric heat generation/absorption term in the energy equation is assumed to be proportional to the high temperature gradient of the form $Q\,\partial T/\partial Y$ as in [12]. To quantify the radiative heat flux, we adopted Rosseland approximation in X and Y-directions modeled as $q_x=-4\sigma/3k'.\partial T^4/\partial X$, $q_y=-4\sigma/3k'.\partial T^4/\partial Y$ where σ is the Stefan-Boltzman constant and k' is the mean absorption coefficient. It is assumed that the temperature differences within the flow are sufficiently small such that T^4 may be expressed as a linear combination of temperature and expand in Taylor's series about T_c and neglecting higher order terms, then $T^4\cong 4TT_c^3-3T_c^4$ evaluated at the temperature T_c, is used to stimulate the effects of thermal radiation as in [10] and [11]. Under these assumptions, the governing equations in dimensionless form are:

$$u_x+u_y=0 \tag{1}$$

$$uu_x+vu_y=-(P-P_c)_x+u_{xx}+u_{yy}-(M+D_a^{-1})u+G_r\theta \tag{2}$$

$$uv_x+vv_y=-P_y+v_{xx}+v_{yy}-D_a^{-1}v \tag{3}$$

$$P_r(u\theta_x+v\theta_y)=\frac{4+3N}{3N}(\theta_{xx}+\theta_{yy})+S\frac{\partial\theta}{\partial y}+J_eE_cu^2+P_rE_c\left[u_y^2+v_x^2+2u_yv_x-4u_xv_y\right] \tag{4}$$

utilised

$$(x,y)=\frac{1}{H}(X,Y),(u,v)=\frac{H}{\upsilon}(u',v'),T_h>T_c$$

$$M=\frac{\sigma_eB_0^2H^2}{\rho\upsilon},G_r=\frac{\beta g(T_h-T_c)H^3}{\upsilon^2},P_r=\frac{\mu C_p}{K},$$

$$S=\frac{QH}{K},J_e=\frac{\sigma_eB_0^2H^2C_p}{K},E_c=\frac{\upsilon^2}{C_p(T_h-T_c)W},$$

$$D_a=\frac{k^*}{H^2},N=\frac{Kk'}{4\sigma T_c^3},\theta=\frac{T-T_c}{T_h-T_c}$$

$$P=\frac{p'H^2}{\rho\upsilon^2},P_c=\frac{p_c'H^2}{\rho\upsilon^2},\lambda=k_wH,\varepsilon=\frac{\varepsilon^*}{H},$$

where H is the channel width, M is the magnetic field parameter, S is the temperature gradient heat generation parameter, D_a is the permeability of the porous medium, N is the radiation parameter, G_r

is the free convection parameter, E_c is the Eckert number and J_e is the Joule heating. The approprate boundary conditions for the considered flow with two wall slip phenomena are:

$$u = 0, v = 0, \theta = h_T \frac{\partial \theta}{\partial y} \text{ at y = } \varepsilon \cos \lambda x \tag{5}$$

$$u = h_2 \frac{\partial u}{\partial y}, v = h_2 \frac{\partial v}{\partial y}, \theta = 1 + h_T \frac{\partial \theta}{\partial y} \text{ at y = 1}$$

Here $h_T = \frac{S_t}{H}$ is the thermal slip, $h_2 = \frac{S_n}{H}$ is the Navier slip, S_t is the thermal slip factor, $S_n = (\frac{2 - m_1}{m_1})\lambda_n$ is the Navier slip factor with m_1 is Maxwell's reflexion coefficient, λ_n means free path and is a constant for an incompressible fluid. A limiting consideration of the solution of the governing equations of the flow is analyzed for $h_T = h_2 = 0$.

3 METHOD OF SOLUTION

We seek perturbation solution for small $\varepsilon << 1$, where the limit $\varepsilon = 0$ is, of course, the limit of a smooth flat wall. We now take the flow field and the temperature to be:

$$u(x, y) = u_0(y) + \varepsilon u_1(x, y), v(x, y) = \varepsilon v_1(x, y)$$
$$P(x, y) = P_0(x) + \varepsilon P_1(x, y),$$
$$\theta(x, y) = \theta_0(y) + \varepsilon \theta_1(x, y) \tag{6}$$

Put (6) in (1)-(5), equating $\varepsilon^0, \varepsilon^1$ and neglecting $0(\varepsilon^2)$, zeroth- and perturbed quantities denoted by the subscripts 0 and 1, respectively, obtained. Eliminate dimensionless P_1 and employ stream function Ψ_1 defined by

$$u_1(x, y) = -\Psi_{1,y}, v_1(x, y) = \Psi_{1,x} \tag{7}$$

Assume wave-like solutions:

$$\Psi_1(x, y) = \varepsilon e^{i\lambda x} \psi(\lambda, y), \theta_1(x, y) = \varepsilon e^{i\lambda x} \phi(\lambda, y) \tag{8}$$

(7) becomes $u_1 = -\varepsilon e^{i\lambda x} \psi'(y), v_1 = \varepsilon i e^{i\lambda x} \psi(y)$, then the perturbed quantities reduced to form of stream function where i is the complex unit. If we further assumed λ to be much less than unit or ($k_w << 1$),

$$\psi(\lambda, y) = \sum_{j=0}^{\infty} \lambda^j \psi_j, \phi(\lambda, y) = \sum_{j=0}^{\infty} \lambda^j \phi_j, (j = 0, 1, 2, ...)$$

And the resulting equations in terms of ψ_j, when compared the like-power terms of λ to the order of λ^2, overall set of coupled nonlinear set of ordinary differential equations and the boundary conditions for this present work are:

$$u_0'' - (M + D_a^{-1}) u_0 = k_p - G_r \theta_0$$
$$(4 + 3N)(3N)^{-1} \theta_0'' + S\theta_0' + J_e E_c u_0^2 + P_r E_c (u_0')^2 = 0 \tag{9}$$

$$\psi_0^{iv} - (M + D_a^{-1}) \psi_0'' = G_r \phi_0'$$
$$(4 + +3N)(3N)^{-1} \phi_0'' + S\phi_0' + 2J_e E_c u_0 \psi_0' - 2P_r E_c u_0 \psi_0 = 0 \tag{10}$$

$$\psi_1^{iv} - (M + D_a^{-1}) \psi_1'' = G_r \phi_1' + i(u_0 \psi_0'' - u_0' \psi_0)$$
$$(4 + 3N)(3N)^{-1} \phi_1'' + S\phi_1' + 2J_e E_c u_0 \psi_1' = 2P_r E_c u_0' \psi_1'' + iP_r (u_0 \phi_0 + \psi_0 \theta_0') \tag{11}$$

$$\psi_2^{iv} - (M + D_a^{-1}) \psi_2'' + D_a^{-1} \psi_0 = 2\psi_0'' + G_r \phi_2'$$
$$i(u_0 \psi_1'' - u_0'' \psi_1)$$
$$(4 + 3N)(3N)^{-1} \phi_2'' + S\phi_2' + 2J_e E_c u_0 \psi_2' - \phi_0 =$$
$$2P_r E_c u_0' \psi_2'' + 2P_r E_c u_0' \psi_0 + \psi_1 \theta_0' + iP_r (u_0 \phi_1 + \theta_0' \psi_1) \tag{12}$$

and

$$u_0 = 0, \theta_0 = h_T \theta_0' \text{ at } y = 0, \tag{13}$$

$$u_0 = h_2 u_0', \theta_0 = 1 + h_T \theta_0' \text{ at y = 1}$$
$$\psi_0' = u_0', \psi_0 = 0, \phi_0 = -\theta_0' + h_T \phi_0' \text{ at y = 0} \tag{14}$$

$$\psi_0' = h_2 \psi_0'', \psi_0 = h_2 \psi_0', \phi_0 = h_T \phi_0' \text{ at y = 1}$$

$$\psi_1' = 0, \psi_1 = 0, \phi_1 = h_T \phi_1' \text{ at y = 0}, \tag{15}$$

$$\psi_1' = h_2 \psi_1'', \psi_1 = h_2 \psi_1', \phi_1 = h_T \phi_1' \text{ at y = 1}$$

$$\psi_2' = 0, \psi_2 = 0, \phi_2 = h_T \phi_2' \text{ ay y = 0} \tag{16}$$

$$\psi_2' = h_2 \psi_2'', \psi_2 = h_2 \psi_2', \phi_2 = h_T \phi_2' \text{ at y = 1}$$

The solutions for the dimensionless axial velocity u, secondary velocity v and temperature field θ satisfying (9) to (12) and the boundary conditions (13) to (16) have been obtained but are not presented here for the sake of brevity. From (6), (7) and (8), after obvious simplification, on the assumption that $\lambda x = \pi/2$, we have $u(x, y) = u_0(y) + \varepsilon \lambda \psi_1'(y)$, $v(x, y) = -\varepsilon \lambda \psi_0(y)$ and $\theta(x, y) = \theta_0(y) - \varepsilon \lambda \phi_1(y)$ and $k_p = (P_0 - P_c)_x$ is the pressure gradient, generate pressure force.

4 RESULTS AND DISCUSSION

The system of non-linear differential equations (9) to (12) with boundary conditions (13) to (16) have been solved in the symbolic computation software MAPLE using mid-point method with Richardson Extrapolation (MMRE). To get a clear insight of the present problem, the numerical results for the u, v and θ have been shown by drawing graphs for different values of the physical paramets, namely, the temperature jump h_T, hydrodynamic slip h_2, forced convection parameter k_p, natural convection parameter G_r, permeability parameter D_a, magnetic field parameter M, radiation parameter N, and heat generation parameter S. The default values of the pa-

rameters in the simulation are: G_r = 2, E_c = 1.5, J_c = 1.5, N = 3, M = 2.5, P_r = 0.71, D_a = 0.3, k_p = 2, h_2 = 0.2, h_T = 0.2 and S = 2 unless otherwise specified. Geometric parameters characterizing the roughness of wall; amplitude ε = 0.025 (characteristic of dilated channel) and wavelength λ = 0.01.

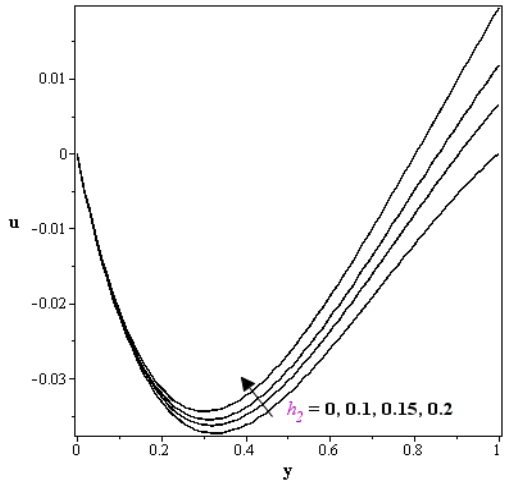

Fig.1 variation of axial velocity u with h_2

Fig.1 shows the impact of h_2 variation on the axial velocity. As h_2 increases, the axial velocity increases at the point y = 0.125 of the channel to the hot flat wall but no effect is noticed at the cool wavy wall. It is obvious in Fig.2 that as h_T increases, the axial velocity increases from the cool wall up to y = 0.736, where it becomes constant, and then decreases towards the hot flat wa ll.

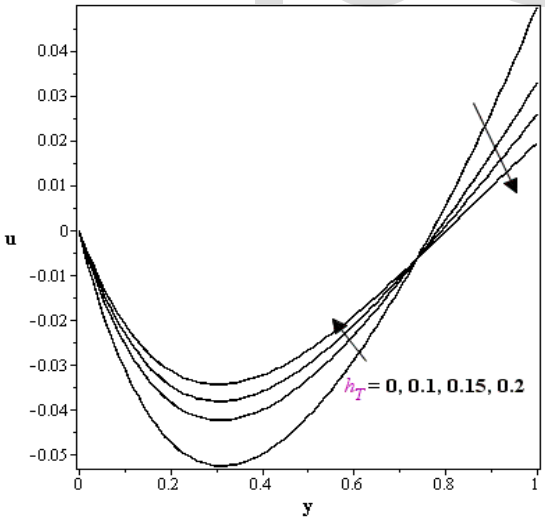

Fig.2 variation of axial velocity u with h_T

In Fig.3 the axial velocity is plotted against y for different values of G_r. Clearly, it is zero at y = 0, which makes the sense in view of boundary condition imposed on the axial velocity and show that the magnitude of u increases steadily for a fixed y up to y = 0.687 in the channel, where it becomes constant in one direction, while towards the hot flat wall u is a decreasing function of y in the opposite direction, while in Fig.4 we noticed a qualitatively similar behavior of opposite trend of u, decreased at $0 \le y \le 0.705$ and increased at $0.705 \le y \le 1$ with an increase in k_p.

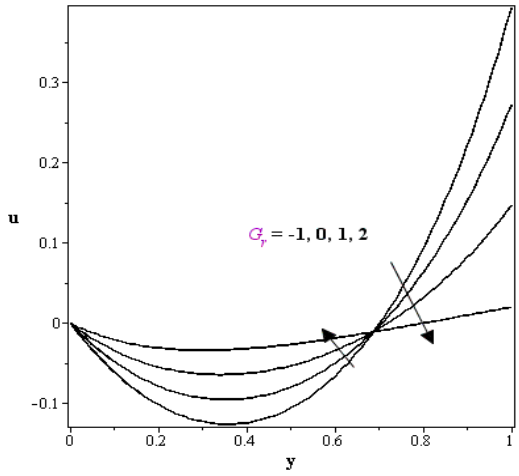

Fig.3 variation of axial velocity u with G_r

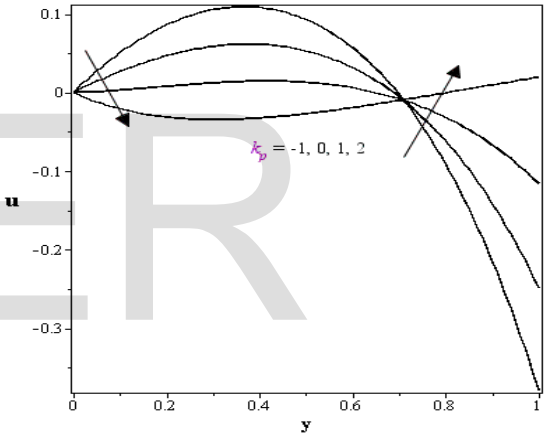

Fig.4 variation of axial velocity u with k_p

Fig.5 gives u at varying values of M due to buoyancy force only and asserts that as M increases the axial velocity of the fluid decrease; attributed to the presence of the transverse magnetic field normal to the walls which gives rise to Lorentz force which is resistive to the flow, hence decelerating axial velocity of the fluid. The flow is find maximal; showing the significant role of natural convection. In Fig.5, it is being observed that u at $0.095 \le y \le 0.787$ of the channel increased but no effect is noticed at the cool wall while it decreased at the hot wall as the fluid flow. Fig.6, Fig.7 reveals an increasing trend of the axial velocity of the fluid in the channel and decrease u at the hot wall while Fig.8 exhibits an opposite trend of the fluid axial velocity with enhancement of M, N and D_a, respectively. Clearly, the axial velocity increases with increasing temperature gradient dependent heat generation parameter S as illustrated in Fig.9.

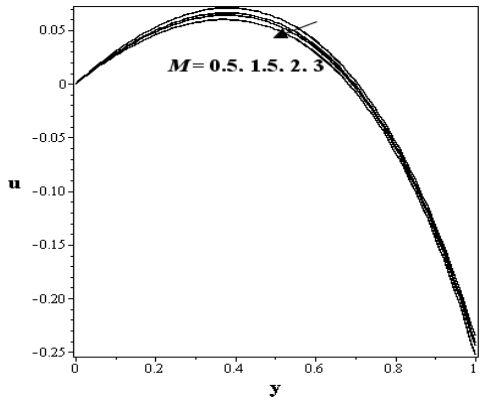

Fig.5 variation of axial velocity u with M: $k_p = 0$, $G_r = 2$

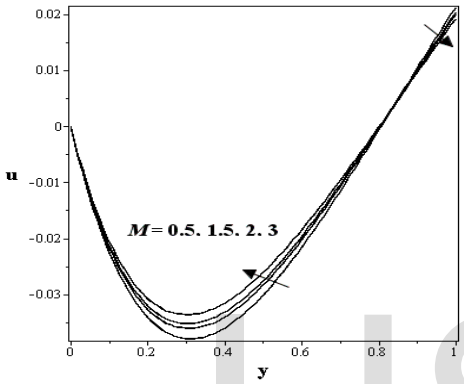

Fig.6 variation of axial velocity u with M: $k_p = 2$, $G_r = 2$

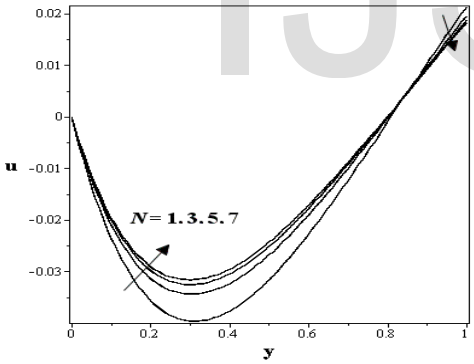

Fig.7 variation of axial velocity u with N

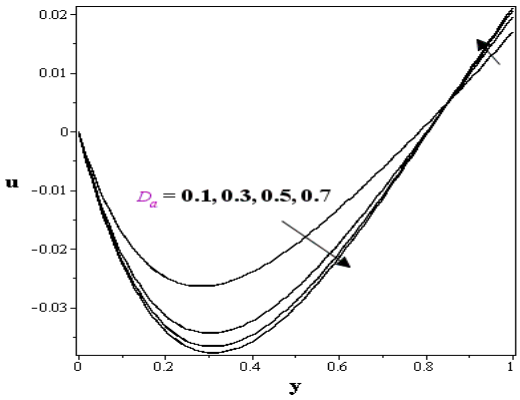

Fig.8 variation of axial velocity u with D_a

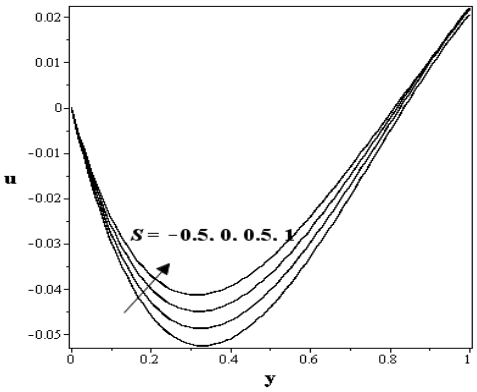

Fig.9 variation of axial velocity u with S

Fig.10 shows the fluid secondary velocity plotted against y for different values of h_2. As h_2 .increases, the fluid secondary velocity decreases at $0.145 \le y \le 0.479$ in the channel. No effect is seen at cool sinusoidal wavy wall but increases is noticed at the hot flat wall while the fluid secondary velocity does not follow a proper pattern at $0.479 \le y \le 0.873$ for change in h_2 .

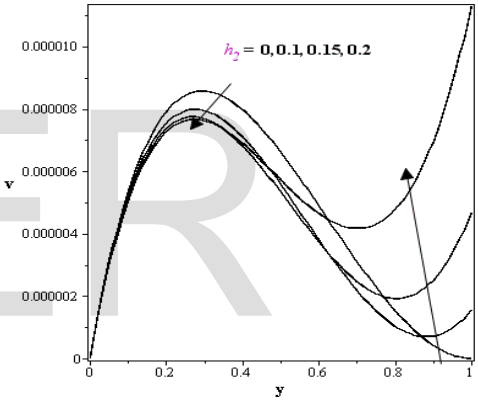

Fig.10 variation of secondary velocity v with h_2

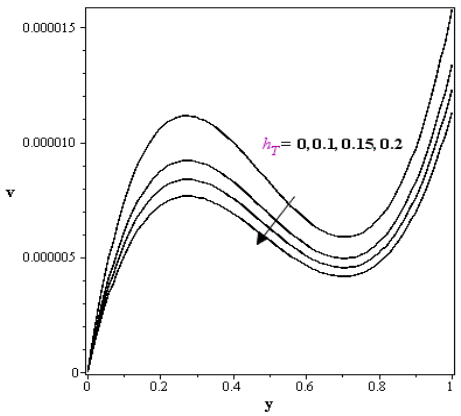

Fig.11 variation of secondary velocity v wth h_T

Fig.11, Fig.12, Fig.13 illustrates the fluid secondary velocity's response to the variation in h_T , G_r , k_p , respectively. Increases in temperature jump, free convection parameter tends to slow down the perpendicular fluid motion and thereby cause decrease in the fluid secondary velocity in one direction, whereas

with the enhancement of forced convection parameter, there is a clear increase in the fluid secondary velocity and negative ve locity is noticed.

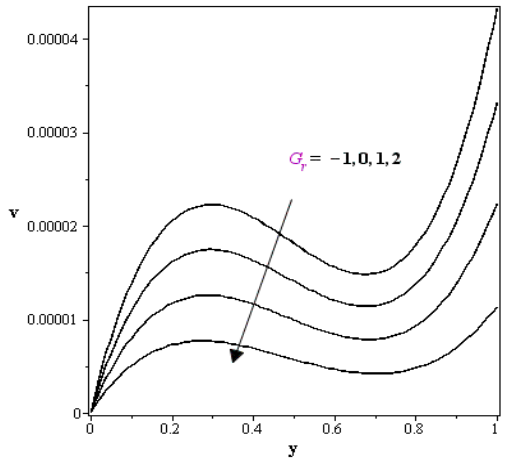

Fig.12 variation of secondary velocity v with G_r

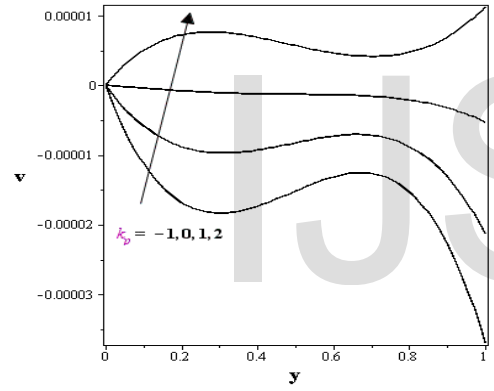

Fig.13 variation of secondary velocity v with k_p

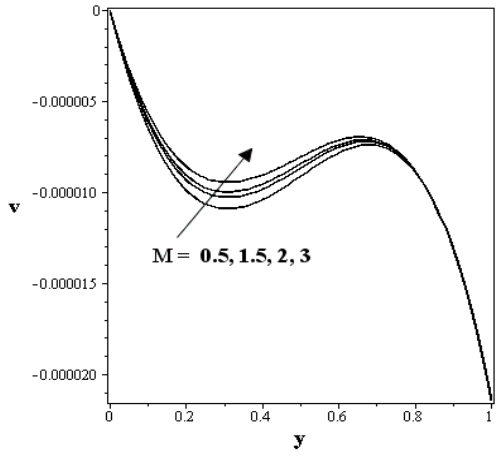

Fig.14 variation of secondary velocity v with M: $k_p = 0,\ G_r = 2$

The impact of M on the fluid secondary velocity is illustrated in Fig.14 represents the case of free convection in the flow field without pressure gradient. It is clear that as M increases, the fluid secondary velocity increases in the channel but no effect on cool and hot walls. We also noticed negative velocity values in the entire channel due to hydrodynamic slip parameter.

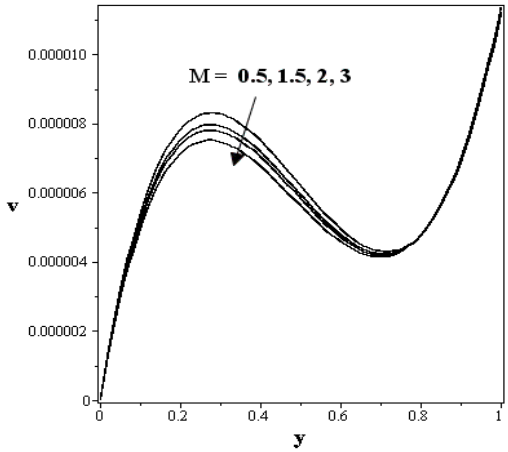

Fig.15 variation of secondary velocity v with M: $k_p = 2,\ G_r = 2$

The magnetic field effect on the fluid secondary velocity is observed in Fig.15 represents general case of convection when a flow is determined where both pressre forces and buoyant forces interact. As M enhanced, the fluid secondary velocity at centre of the channel increases but no impact is seen at both walls.

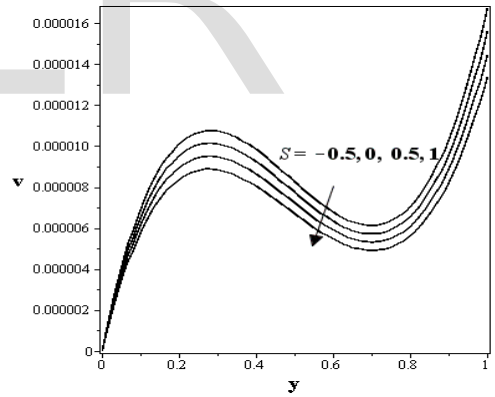

Fig.16 variation of secondary velocity v with S

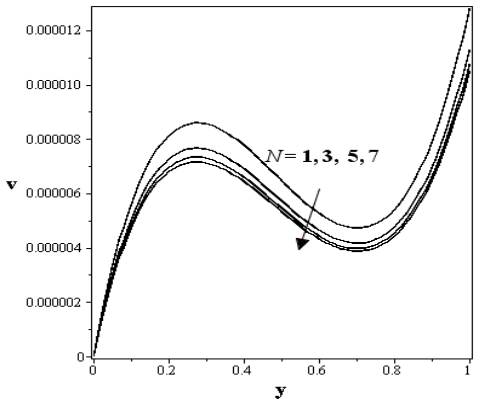

Fig.17 variation of secondary velocity v with N

Fig.16, Fig.17, Fig.18 represents the effect of different values of temperature gradient dependent heat generation parameter S, radiation parameter N, permeability parameter of porous medium D_a, respectively, on the fluid secondary velocity v. v experiences a declination from the position y = 0.089/0.038 to the hot flat wall and no effect is noticed at cool wavy wall (Fig.16/Fig.17) for the growth of S/ N while for the increase in D_a, the v increases to the position y = 0.692 to becomes constant and then diminishing to the hot flat wall (Fig.18). S exert strongest effect on the fluid secondary velocity in comparison with other parameters.

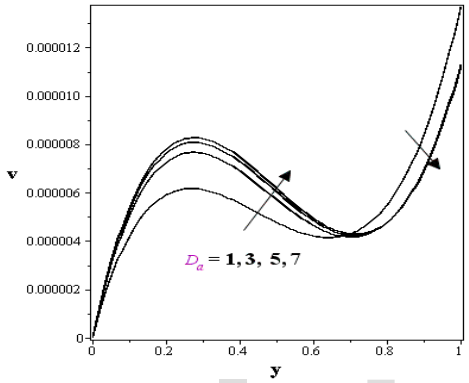

Fig.18 variation of secondary velocity v with D_a

The influence of parameters h_T, G_r, k_p, S and N on the dimesionless temperature distribution θ is shown in Fig.19, Fig.20, Fig.21, Fig.22 and Fig.23, respectively, are presented Here we see that for varied parameter the minimum temperature θ = 0 at the cool sinusoidal roughened wall and different maximum temperature at the hot flat wall. This indicates variation of temperature due to temperature jump. It is clear in Fig.19 that the fluid temperature increased throughout the channel width due to thermal slip. The fluid temperature enhanced up significantly (Fig.20, Fig.21) towards the hot flat wall for higher values of G_r and k_p but no effect is observed at cool wall.

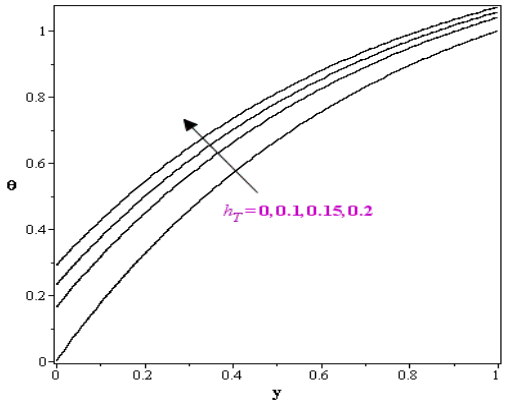

Fig.19 Temperature profiles θ for different values of h_T

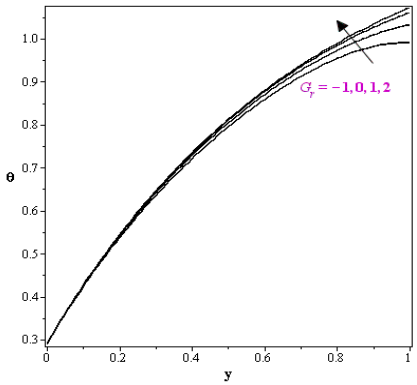

Fig.20 Temperature profiles θ for different values of G_r

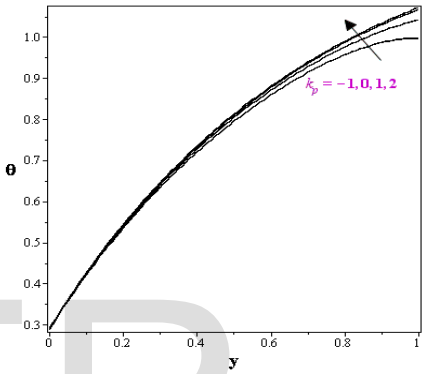

Fig.21 Temperature profiles θ for different values of k_p

Fig.22/Fig.23 reveals an increasing trend of the fluid temperature distribution with the enhancement of S/N at y = 0 up to around y = 0.775/0.798, where it becomes constant and then decelerating down and decreases to the hot flat wall. The temperature gradient dependent heat generation parameter S exert stronger effects on the temperature profiles in comparison with radiation parameter. We observed that the parameters h_2, M and D_a have insignificant influence on temperature distribution. For this reason, no figure for the h_2, M and D_a on temperature field are presented herein.

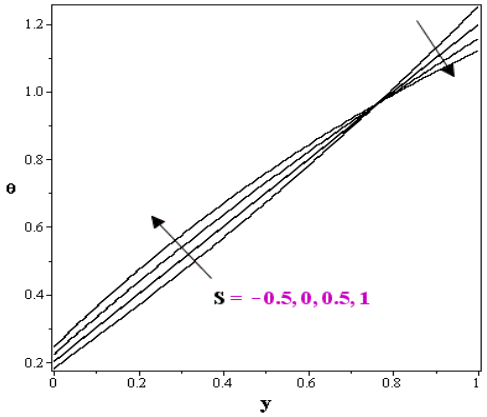

Fig.22 Temperature profiles θ for different values of S

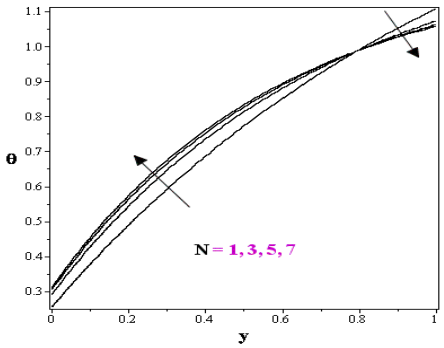

Fig.23 Temperator profiles θ for different values of N

5 CONCLUSION

The mathematical modeling of mixed convection flow through a channel with dilated ($:\varepsilon > 0$)-constricted ($:\varepsilon < 0$) geometries; there is more intimate contact between them, augment the transportation of energy and momentum, is carried out. Finitely long vertical sinusoidal wavy channel with two slip phenomena and amplitude parameter ε; characterizing the roughness of the wall, on the flow fields is employed. The flows spread out larger; both axially (primary) and transversely (secondary), with the secondary velocity being towards the axis in the fluid bulk rather than restricting or confining within a thin layer as in fully developed flow through vertical channel. This is relevant in energy and material saving considerations as the geometry stands to improve the design of heat exchanger equipment. From the results and discussions that follow subsequent outcome are drawn as:

- The fluid axial velocity shows flow reversal due to a velocity slip and a resistive force of pressure gradient. It shows increase-decrease trends for h_T, D_a, M and N and exhibits opposite trend for k_p and D_a
- Fluid secondary velocity was skewed to irregular flow pattern because of the application of combined convection that creates a resistive force that acts in different direction to the fluid motion as h_2 increases. It decreases with increasing values of h_T, G_r, M, N and S, increases with increasing k_p, and increase-decrease as D_a increases.
- Fluid temperature increases remarkably in the entire channel width with increasing h_T while seeing increases only near the hot wall with increasing G_r and k_p, and h_2, M and D_a have no effect on temperature. S/N enhancement causes the temperature increase from cool wall up to a point y = 0.775/0.798 and then decrease towards the hot wall.

REFERENCES

[1] S. Parvin, M.A. Alim and N.F. Hossain, "MHD mixed convection heat transfer through vertical wavy isothermal channels," Int. J. of Energy & Tech., vol. 3, no. 34, pp. 1-9, 2011.

[2] D.S. Chauhan and R. Agrawal, "Magnetohydrodynamic convection effects with viscous and Ohmic dissipation in a vertical channel oartially filled by a porous medium," J. of Appl. Sci. and Eng., vol. 15, no. 1, pp. 1-10, 2012.

[3] R. Patra, S. Das and R.N. Jana, "Radiation effect on MHD fully developed mixed convection in a vertical channel with asymmetric heating," J. of Appl. Fluid Mech., vol. 7, no. 3, pp. 503-512, 2014.

[4] K. Vajravelu and K.S. Sastri, "Free convective heat transver in a viscous incompressible fluid confined between a long vertical wavy wall and a parallel flat wall," J. of Fluid Mechs., vol. 86, no. 2, pp. 365-383, 1978.

[5] P.F. Fasogbon, "MHD flows in corrugated channel," Int. J. of Pure and Appl. Maths., vol. 27, no. 2, pp. 227-239, 2006.

[6] P.F. Fasogbon, "Analytical studies of heat and mass transfer by free convection in a two-dimensional irregular channel," Int. J. of Appl. Math. and Mech, vol.6, no.4, pp. 17-37, 2010.

[7] J.A. Gbadeyan, T.L. Oyekunle, P.F. Fasogbon and J.U. Abubakar, "Soret and Dufour effects on heat and mass transfer in chemically reacting MHD flow through a wavy channel," J. of Taibah university for Sci., vo l. 12, no. 5, pp. 631-651, 2018.

[8] R. Taneja and N.C. Jain, "MHD flow with slip effects and temperature-dependent heat source in a viscous incompressible fluid confined between a long vertical wavy wall and a parallel flat wall," Defence Sci. J., vol. 54, no. 1, pp. 21-29, 2004.

[9] K.D. Singh, "MHD mixed convection visco-elastic slip flow through a porous medium in a vertical porous channel with thermal radiation," Kragujevac J. Sci., vol. 35, pp. 27-40, 2013.

[10] S. Sengupta and N. Ahmed, "MHD free convective chemically reactive flow of a dissipative fluid with thermal diffusion, fluctuating wall temperature and concentrations in velocity slip regime," Int. J. of Appl. Math and Mech., vol. 10, no. 4, pp. 27-54, 2014.

[11] S. Jana and K. Das, "Influence of variable fluid properties, thermal radiation and chemical reaction on MHD slip flow over a flat plate," Italian J. of Pure and Appl. Math., no. 34, pp. 29-44, 2015.

[12] S.M. Ibrahim and K. Suneetha, "Effects of thermal diffusion and chemical reaction on MHD transient free convection flow past a porous vertical plate with radiation, temperature gradient dependent heat source in slip flow regime," J. of Computational and Appl. Res. in Mechanical Engineering , vol. 5, no. 2, pp. 83-95, 2016.

[13] C.H. Amanulla, N. Nagendra and M.S. Reddy, "Thermal and momentum slip effects on hydromagnetic convection flow of a Williamson fluid past a vertical truncated cone," Frontiers in heat and Mass transfer, vol. 9, no. 22, pp. 1-9, 2017.

[14] N. Nagendra, C.H. Amanulla and M.S. Reddy, "Slip effects on MHD flow of a Williamson fluid from an Isothermal Sphere: A numerical Study," AMSE JOURNALS-AMSE IIETA publication-2017-Series: Modelling B; vol. 86, no. 3, pp. 782-807, 2018.

[15] I.G. Baoku, "Influence of chemical reaction, viscous dissipation and joule heating on MHD Maxwell fluid flow with velocity and thermal slip over a stretching sheet," J. of Advances in Math. and computer science, vol. 28, no. 1, pp. 1-20, 2018

[16] K.R. Sekhar, G.V.R. Reddy and B.D.C.N. Prasad, "Chemically reacting on MHD oscillatory slip flow in a planer channel with varying temperature and concentration," Advances in Appl. Sci. Research, vol. 3, no. 5, pp. 2652-2659, 2012.

[17] M.J. Uddin, A. Beg and M.N. Uddin, "Multiple slip and variable transport peoperty effects on magnetohydromagnetic dissipative thermo-solutal convection in porous media," ASCE J. of Aerospace Eng. 2016. http:usir.salford.ac.uk/399096/